Optimization of Uniformity for Current Polar Drive Implosion Experiments on the National Ignition Facility

E. M. Garcia

Penfield High School

Advisor: Dr. R. S. Craxton

Laboratory for Laser Energetics

University of Rochester

Rochester, NY

October 2014

1. Abstract

Several types of alternative designs for the current series of polar drive implosions on the National Ignition Facility (NIF) have been developed using the hydrodynamics simulation code *SAGE*. Polar drive is a method of repointing the NIF beams, which are configured for indirect drive, away from the poles and towards the equator to create a uniform direct drive implosion. The current design produces implosions that are close to spherical but still show some nonuniformities. They are calculated to have a center-of-mass nonuniformity of 1.3% averaged over the whole sphere when the shell has compressed to approximately half its initial diameter. The first alternative design, the "defocus" design, utilizes greater defocuses than the current design on all of the beams along with small changes to the pointing shifts. This design has a lower nonuniformity of 0.64%. The second type of alternative design, the "oblique" design, uses large pointing shifts so that most beams encounter the target at oblique incidence. It is speculated that the large pointing shifts of oblique designs may help to reduce the nonuniformity associated with laser speckle that is not modeled in the simulations. All beams in the oblique designs have a minimum pointing shift of 45% of the target radius. One oblique design has an rms nonuniformity of 0.57% and the other an rms nonuniformity of 0.64%. The final two alternative designs are optimized to overdrive the equator of the target by a small amount to allow for fine tuning of NIF experiments and demonstrate the ability of polar drive to overdrive the equator of the target if desired.

2. Introduction

Controlled fusion is a potential abundant source of clean, safe energy. One method to create fusion is to irradiate a spherical target consisting of a plastic or glass shell filled with deuterium and tritium with powerful lasers. The energy from the lasers causes the shell of the

target to ablate outwards while at the same time compressing the deuterium fuel inside the target. The high temperature and pressure at the core of the compressed target create an environment in which Coulomb repulsion forces between nuclei can be overcome and fusion reactions can occur for a short time until the target explodes. As deuterium and tritium nuclei fuse, they form a helium nucleus and an energetic neutron, which carries most of the energy from the fusion reaction. If the fuel has a great enough radius and density, the energy from the helium nucleus will be redeposited in the fuel. This redeposition of energy is known as ignition and is the first step towards breakeven, when the energy released by fusion is equal to the energy input of the laser. Breakeven is a step towards high gain, which is when the energy output is substantially higher than the energy input. High gain is necessary for laser fusion to be used as an abundant energy source.

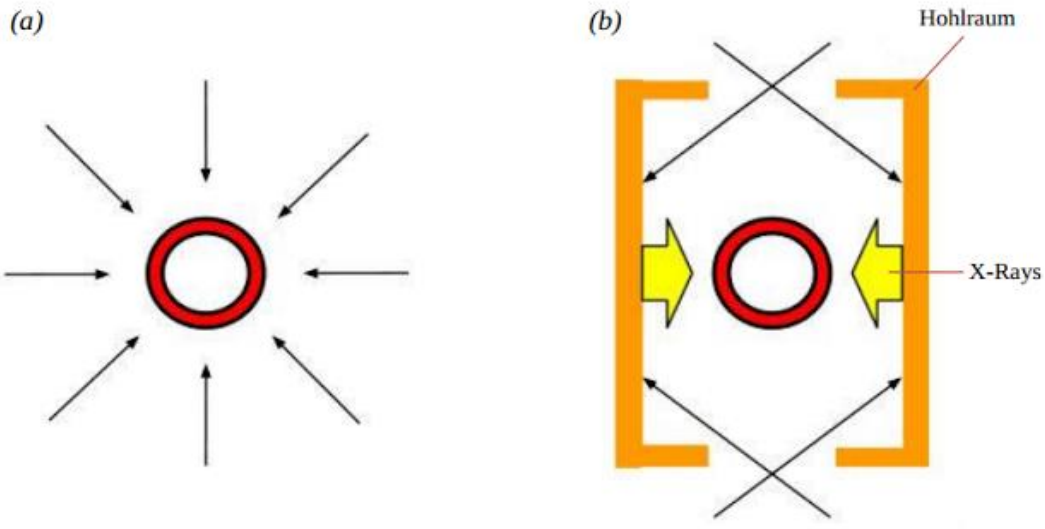

Figure 1: The two main approaches to inertial confinement fusion. (a) In direct drive, the target is irradiated directly by a symmetrical set of beams, represented by the black arrows. (b) In indirect drive, the laser beams irradiate a cylindrical hohlraum made of a metal with a high atomic number (usually gold) surrounding the target, which then emits x rays (yellow block arrows) that irradiate the target. (From Reference 1)

There are two main approaches to laser fusion currently being used: direct drive[2] and indirect drive[3]. In direct drive [Figure 1 (a)], a target is irradiated directly with laser beams coming in at normal incidence from all directions in a symmetrical configuration. The OMEGA laser at the University of Rochester's Laboratory for Laser Energetics (LLE) is configured to perform direct drive experiments. In the indirect drive approach, a cylindrical hohlraum made of a metal with a high atomic number, usually gold, is placed around the target, and the laser beams enter the hohlraum through holes at the top and bottom and irradiate the inside of the cylinder [Figure 1 (b)]. The hohlraum then re-emits about 80% of the energy it absorbed as x rays, some of which irradiate the target. This approach has the advantage of irradiating the target with good uniformity. However, only 20% of the energy from the laser beams is actually absorbed by the target, making this an inefficient method of fusion. The National Ignition Facility (NIF) at Lawrence Livermore National Laboratory is configured for indirect drive.

Because the NIF is set up to perform indirect drive experiments, the beam ports aren't located in ideal places to perform direct drive experiments. The NIF has 48 beam ports available evenly spaced around the azimuth (Φ) at angles of Θ = 23.5°, 30.0°, 44.5°, and 50.0° from the poles, with corresponding angles in the lower hemisphere. Each port is used by 4 beams called a quad, for a total of 192 beams. If the NIF beams are pointed at the center of the target in a direct drive experiment, the poles are drastically overdriven in comparison to the equator, which is inadequate as it doesn't provide enough compression of the fuel to generate a lot of fusion reactions [Figure 2 (a)]. To create uniform direct drive implosions on the NIF, a method of repointing the beams called polar drive[4,5,6,7] is used [Figure 2 (b)]. In this method, some of the beams are pointed towards the equator so that they no longer encounter the target at normal incidence and instead deposit their energy near the equator.

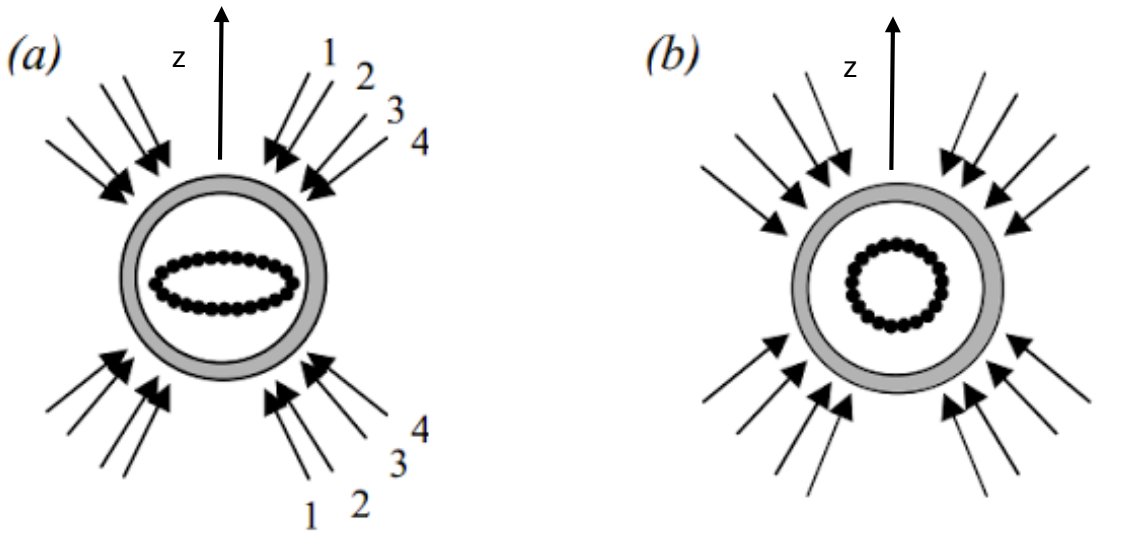

Figure 2: Possible pointings of NIF beams for direct drive implosions. Quads are indicated by the numbers next to the arrows. Quad 1=23.5°from the z axis, Quad 2=30.0°, Quad 3=44.5°, and Quad 4=50.0°. (a) When all beams are aimed at the center of the target, the shell implodes faster at the poles than at the equator. (b) Repointing the beams away from the center of the target and towards the equator creates a more uniform implosion. Based on figure 2 of reference 8.

This type of pointing scheme has been effective in current direct drive experiments on the NIF carried out by LLE[7]. The purpose of this work was to improve upon the uniformity of the existing polar drive design using a variety of approaches, as nonuniformities are still observed in different types of images of current polar drive implosions.

3. Current Design

The target that is being used for current polar drive implosions on the NIF is a 1100 μm radius target with a plastic shell that is 100 μm thick [Figure 3 (a)]. The shell is filled with deuterium. The laser pulse shapes for each quad were already optimized for the current design[7] and were different for each ring of quads. The pulse shapes were not changed in this work. A diagram of the average pulse shape as well as the absorption for the current design is shown in Figure 3 (b).While good absorption is obtained at early times, it is difficult to keep a high

absorption percentage at later times because some energy misses the target as the shell compresses.

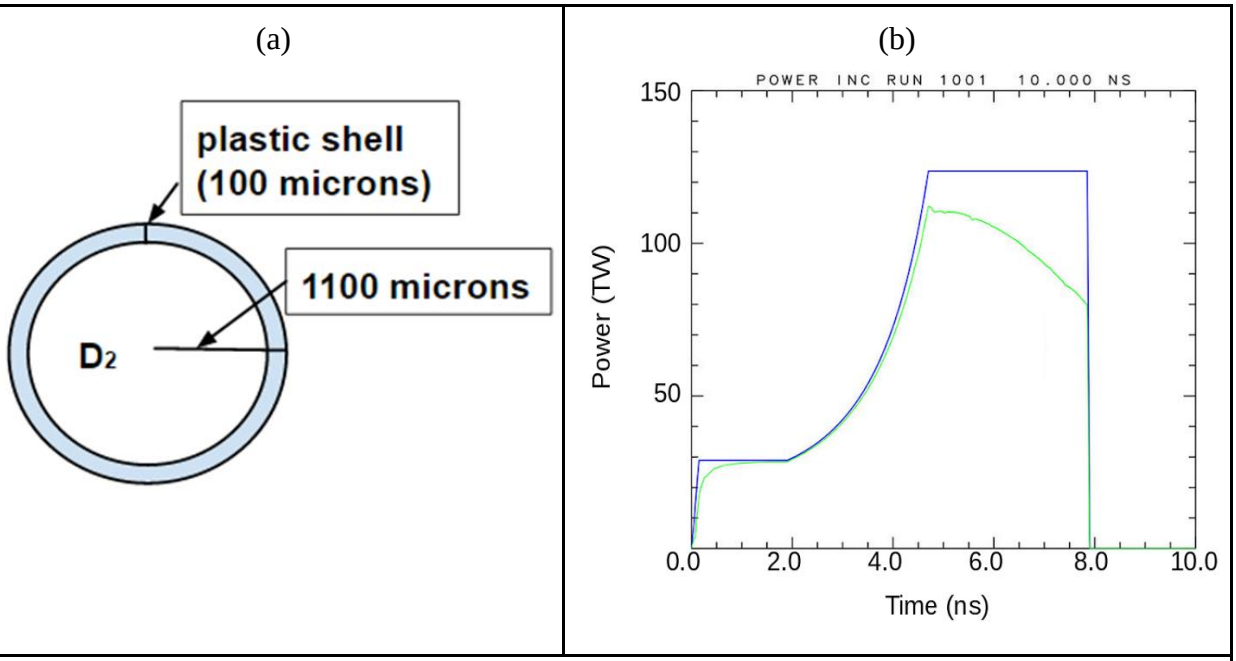

Figure 3: (a) Diagram showing the target simulated in these designs. (b) Laser power incident (blue) and absorbed (green) as a function of time. The blue line shows the pulse shape, which increases in intensity in the second half of the pulse. The green line shows the absorbed power, which decreases as the target compresses.

Three main parameters can be manipulated in developing a design [figure 4]. The defocus of a beam can be changed by moving the lens towards the target, which creates a larger laser spot. Some degree of defocus is required for polar drive designs because NIF phase plates create a tighter focus in order to allow the beams to pass through the hole in the hohlraum. The aim point of a beam can be changed by moving a mirror. Finally, the energy in each beam can also be specified. The use of these parameters to make polar drive implosions viable on the NIF using indirect drive phase plates was first described in Reference 8. The hydrodynamics code SAGE was used to model these parameters and their effects on the target implosion.

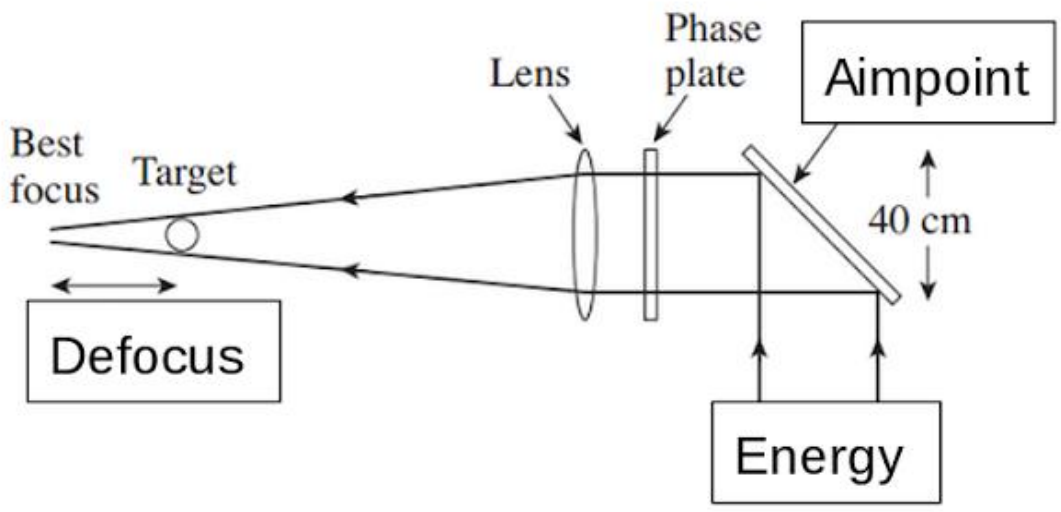

Figure 4: Diagram showing the parts of the NIF setup that allow for the changes in the parameters described in these designs. The defocus can be changed by moving the lens closer to the target, and the aim point can be changed by moving the mirror. The energy coming into this system for each quad can also be adjusted. All designs discussed in this paper use the NIF's indirect drive phase plates. (Based on Figure 3(a) of Reference 8)

The design currently being used for the polar drive implosions carried out by LLE on the NIF uses small defocuses on all beams and pointings that are close to the laser ports, especially for quads 1, 2, and the top beams of quad 3. It has several good qualities. First, it has a high absorption of 85.7% [Figure 3]. It also achieves good uniformity and has an rms of 1.30%. It is possible to see the potential source of some remaining nonuniformities by looking at the *SAGE* model of these implosions. Figure 5 shows a center-of-mass radius contour plot of the current design. Contours show deviations from the average center-of-mass radius, squares show the location of beam ports, dots show the beam aim points, and arrows show a selection of beam pointings. It can be observed from this plot that this design still contains some prominent features such as azimuthal nonuniformities around Θ=60°. Even with these features, the overall nonuniformity of this design as modeled by *SAGE* is only 1.30%. However, it is believed that an

rms of at most 1.0% is required for ignition, so there was a need for improvements to the current design.

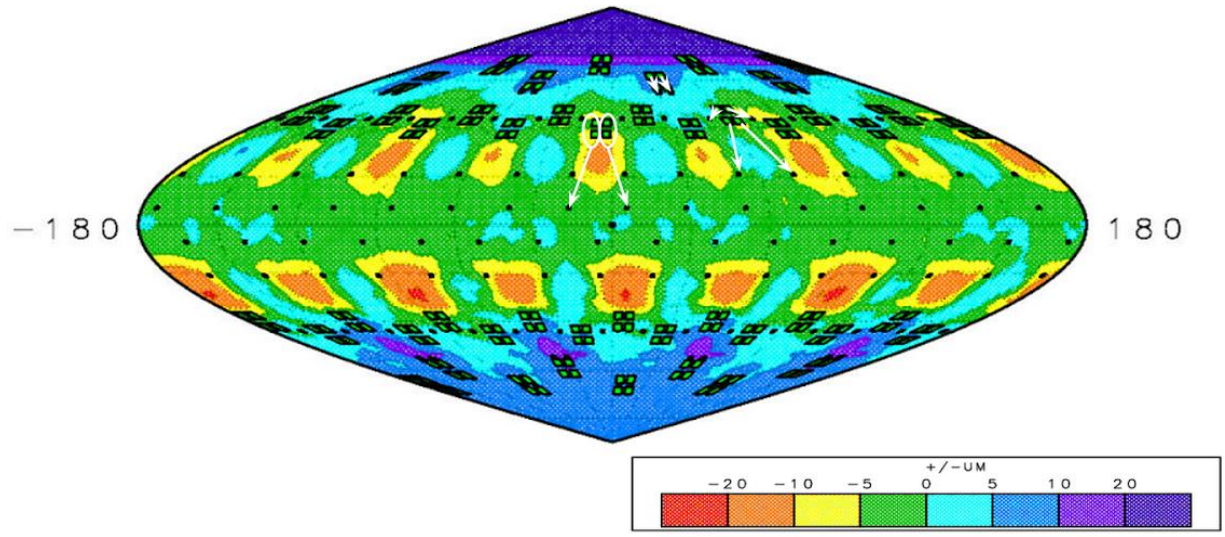

Figure 5: *SAGE* center-of-mass radius contour plot showing deviations from the mean radius in μm and pointings of the current design at 6 nanoseconds when the target's radius has been compressed from 1100 to 631 μm. The quad 1, quad 2, and upper quad 3 beams are pointed close to their origin, but the lower quad 3 and all quad 4 beams have large repointings towards the equator as well as horizontal shifts. These are specified as aim points on the target surface. The most visible features in this plot are the large fluctuations in radius around Θ=60°, which are likely caused by the small defocuses. This design has an RMS nonuniformity of 1.30%.

Nonuniformities in the current design are also evident in different types of images of current polar drive implosions. One type of diagnostic imaging that has been used on the NIF to determine how uniformly the targets for the current design implode is self-emission. Self emission captures the x rays given off by the outside of the shell as it implodes. In self emission imaging [Figure 6 (a)] the implosion seems to be fairly uniform, but it is evident that the areas around Θ=60°and Θ=120° appear to be slightly under compressed, creating a slight hexagonal shape. However, when another type of imaging known as x ray backlighting is used, nonuniformities become much more prominent [Figure 6 (b)]. In x ray backlighting, a secondary

target is shot to produce x rays, which pass through the primary target and reach a detector. The bright areas in the image are where x rays are being detected, and the dark shadow traced by the white line is where the shell of the primary target is blocking the x rays, allowing the nonuniformities in the dense shell to be seen. The nonuniformities visible from this type of imaging warrant further improvements to the uniformity of polar drive designs.

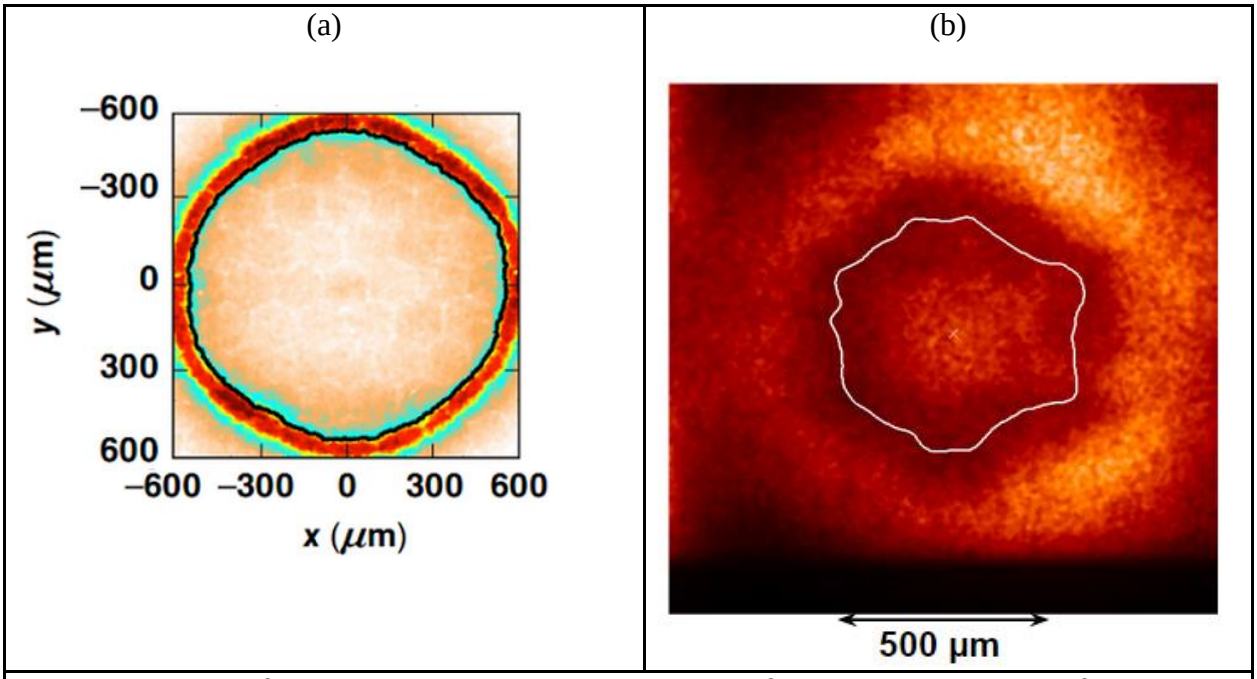

Figure 6: Images of the current design on the NIF viewed from the equator. (a) Self emission image[9]. While close to spherical, it is still possible to see a slight hexagonal shape. (b) X ray backlighter image[10]. In a backlit implosion of the current design, it is much easier to see some nonuniformities in the imploding shell.

4. Optimized Designs

Three types of optimized designs were developed, each with a different goal. The defocused design had a goal of reducing the RMS nonuniformity of the original design using similar pointings and larger defocuses. The oblique designs had the goal of creating a pointing scheme that gives every beam as big of a shift as possible while maintaining good uniformity. Finally, the overdriven equator designs had a goal of overdriving the equator by a certain

amount. Because nonuniformities in the shell seeded at early times grow as time goes on, measurements of rms nonuniformity were taken at 6 nanoseconds when the target had been compressed to about half its initial radius (about 630 μm).

Every beam in each quad could be given its own shift in both the Θ and Φ directions. This allowed for flexibility in the distribution of energy. Because designs that are symmetrical around the azimuth were desired, parameters were specified for one quad in each ring and copied to the other quads in each ring.

4 a. Defocused Design

The first goal of the optimization process was to create a design that used bigger defocuses to spread out the energy from each beam more and therefore increase the overall uniformity. The effect of larger defocuses can be seen in Figure 7, which shows the energy deposition of a single beam with a small (1 cm) and large (2.6 cm) defocus, and Figure 8, which shows how the shape of a beam changes as it is defocused. In addition to spreading the energy over a larger area, defocusing the beams creates a more gradual falloff from the maximum deposited energy for each beam and a lower maximum energy. Both of these features make it much easier to overlap beam energies to create a smoother implosion overall. In the process of optimizing this type of design it was observed that simply increasing the defocuses of the current design without any repointings resulted in an overdriven equator, which led to the group of designs meant to overdrive the equator discussed in section 4 c. Because of this, small pointing shifts from the current design were used in the defocused design along with the larger defocuses. Larger defocuses cause some loss of energy, so a 7% increase in energy from the current design was applied to all beams to ensure that the target is imploded to the same radius at the same time for both designs.

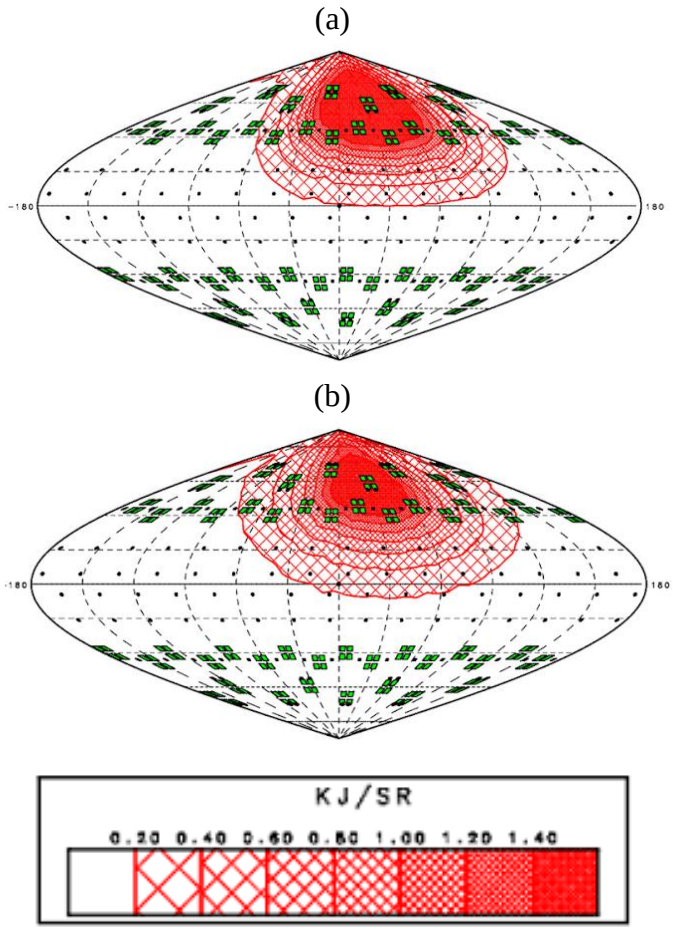

Figure 7: Energy deposition of a quad 2 beam in kJ/sr for the current design with a defocus of 1.0 cm (a) and the defocused design with a defocus of 2.6 cm (b). The small defocus concentrates most of the energy in a smaller area and creates a steep falloff of energy deposition, while the large defocus has a more gradual falloff.

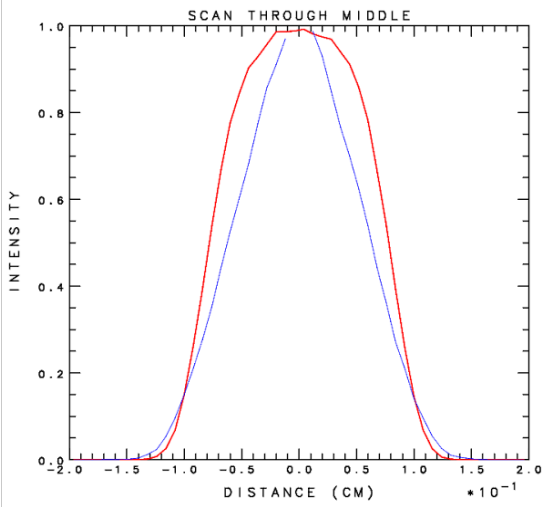

Figure 8: Normalized lineout in the horizontal direction showing the shape of a quad 2 beam defocused to 1.0 cm (red) and 2.6 cm (blue). The intensity of the beam falls off much more gradually in the beam defocused 2.6 cm than in the beam defocused 1.0 cm.

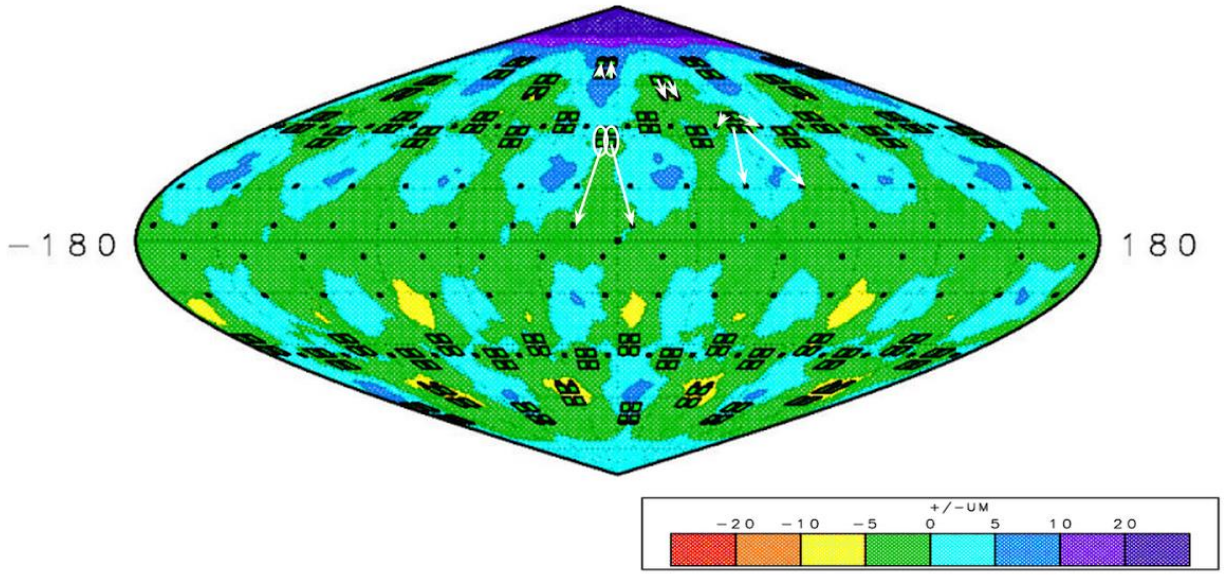

Figure 9: *SAGE* center-of-mass radius contour plot showing deviations from the average radius in μm and pointings of the defocused design at 6 nanoseconds when the target has been compressed to 629 μm. The defocused design has an rms nonuniformity of 0.64%. Top/bottom asymmetries are caused by noise in the code.

The defocused design is shown in figure 9 at 6 nanoseconds. The azimuthal nonuniformity around Θ=60° is greatly reduced in this design. The uniformity in the Θ direction is also much better in this design. The slight difference between the northern and southern hemispheres is caused by noise in the code and the fact that the contour levels have very small increments. Overall, this design has an rms nonuniformity of 0.64%. This is well below the 1.0% rms thought to be required for ignition. The parameters used in the defocused design are shown in Table 1.

	Defocused Design			Oblique Design		
Beam	Defocus (cm)	Theta (°)	Delta Phi (°)	Defocus (cm)	Theta (°)	Delta Phi (°)
1	2.4	20	0	3.0	23	70
2	2.4	20	0	3.0	23	115
3	2.4	20	0	3.0	23	-115
4	2.4	20	0	3.0	23	-70
5	2.6	35	0	2.7	39	70
6	2.6	35	0	2.7	39	115
7	2.6	35	0	2.7	39	-115
8	2.6	35	0	2.7	39	-70
9	2.0	46	-11.25	1.8	48	35
10	2.0	46	11.25	1.8	48	60
11	2.0	69	-11.25	1.8	68	-60
12	2.0	69	11.25	1.8	68	-35
13	1.8	84	-11.25	1.8	81	-11.25
14	1.8	84	11.25	1.8	81	11.25
15	1.6	84	-11.25	1.8	81	-11.25
16	1.6	84	11.25	1.8	81	11.25
17-32	all parameters a reflection of upper hemisphere			all parameters a reflection of upper hemisphere		

Table 1: Parameters of the defocused and first oblique designs. All beams in the defocused design also have an energy increase of 7% from the current design, and beams in the first oblique design have an energy increase of 25% from the current design. Beam 1 is the top left beam in Quad 1, Beam 2 is the top right beam in Quad 1, Beam 3 is the bottom left, etc.

4 b. Oblique Designs

One source of nonuniformities that isn't accounted for in the *SAGE* models is laser speckle. As illustrated in Figure 10, laser beams have areas of higher and lower intensity caused by the way the beam focuses and interferes with itself after going through a phase plate. At late times this speckle is smoothed out more by thermal conduction because the energy is absorbed farther out in the corona of the target, but at early times this speckle can create divots in the target surface known as imprint that don't smooth out as the target implodes [Figure 10 (a)]. It is speculated that having beams encounter the target at oblique incidence could help reduce this imprint by spreading energy over a larger area and by depositing energy farther from the critical surface even at early times [Figure 10 (b)]. In addition, oblique rays will deposit their energy over a larger area as they refract through the plasma, in contrast to normal incidence rays which deposit their energy at a single point on the target shell.

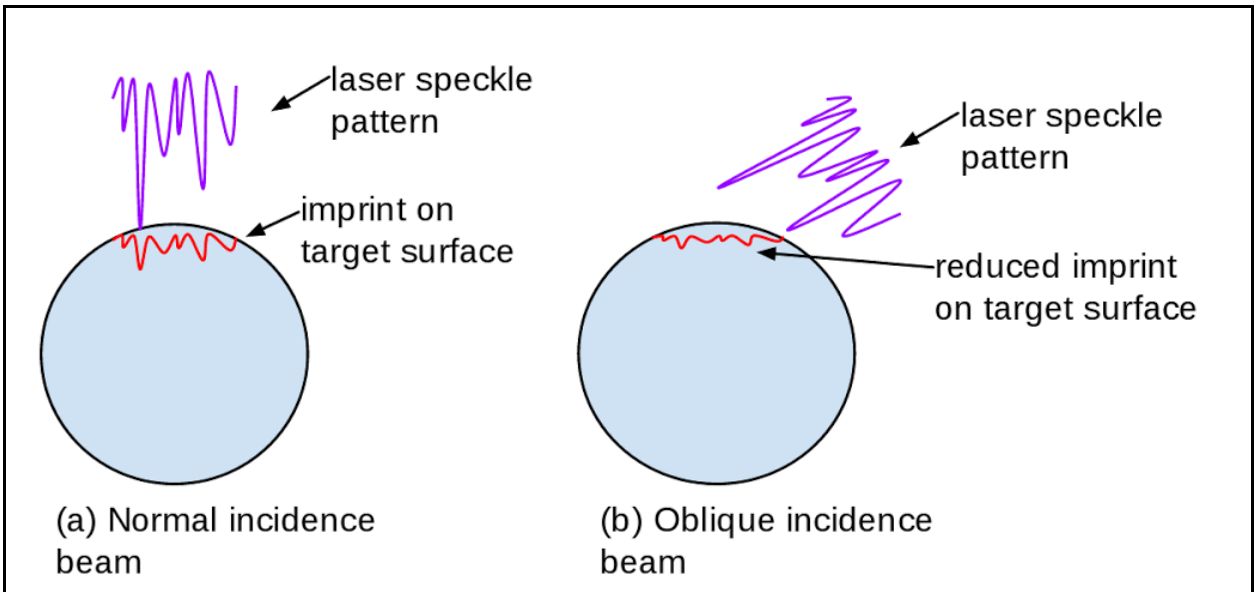

Figure 10: Diagram showing how laser speckle influences uniformity. (a) A normal incidence beam creates an exaggerated imprint pattern. (b) An oblique incidence beam is speculated to reduce imprint on the target surface.

The first oblique design was developed with the goal of having large total pointing shifts for all beams. In the design, all beams have a total pointing shift between 495 and 932 μm, or at least 45% of the target radius. This design has similar defocuses to the defocused design. To gain the benefits of the oblique beams with respect to speckle, every beam in quads 1-3 was given a shift in the Φ direction, spreading out the energy and increasing the uniformity of the energy deposition on the target. Quad 4 beams weren't given an additional azimuthal shift because they already have a large shift in the Θ direction. As seen in figure 11, this design gives a good overall uniformity of 0.57%.

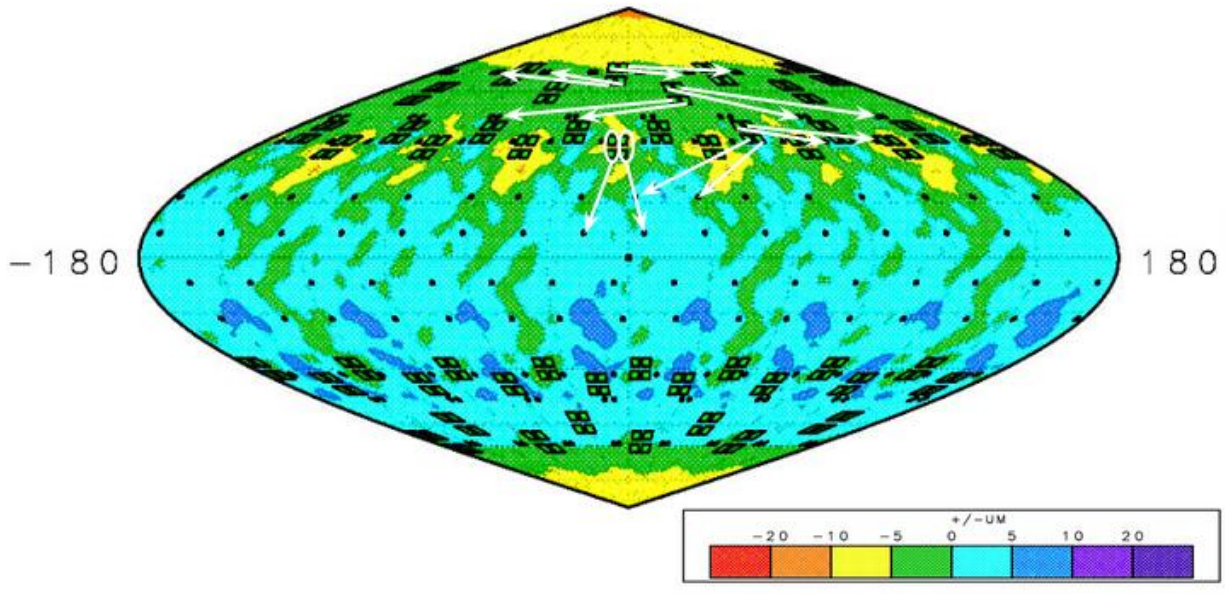

Figure 11: *SAGE* center-of-mass radius contour plot showing deviations from the mean radius in μm and pointings of the first oblique design when the target has been compressed to 632 μm. This design has an rms nonuniformity of 0.57%.

The effects of an oblique pointing on energy deposition can be seen in Figure 12, which shows the energy deposition pattern of a repointed beam in kJ/sr. With an oblique pointing, the majority of the laser's energy is deposited far away from the laser port, and very little energy

encounters the target at normal incidence. The one disadvantage to this design is that it requires a 25% increase in energy from the original design to compress to the same radius at the same time, since oblique beams with large defocuses experience reduced absorption. This occurs because while most of the energy hits the target at early times, as the target implodes it decreases in size and some energy will miss the target [Figure 13].

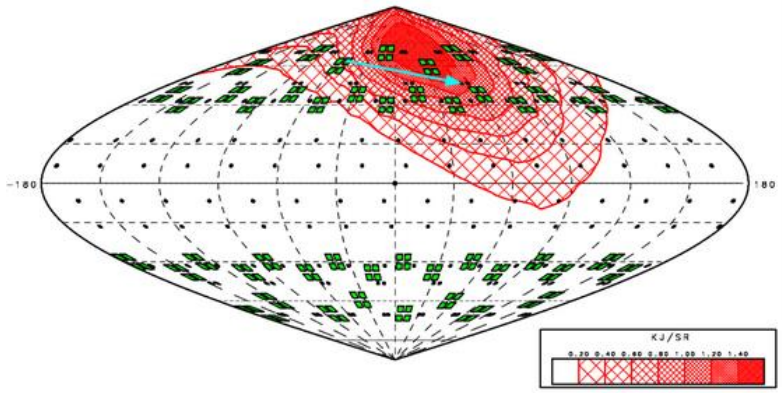

Figure 12: Energy deposition of a quad 2 beam in the first oblique design in kJ/sr. The blue arrow shows the pointing shift of the beam. The majority of the energy is deposited far away from the laser port, with very little energy encountering the target at normal incidence.

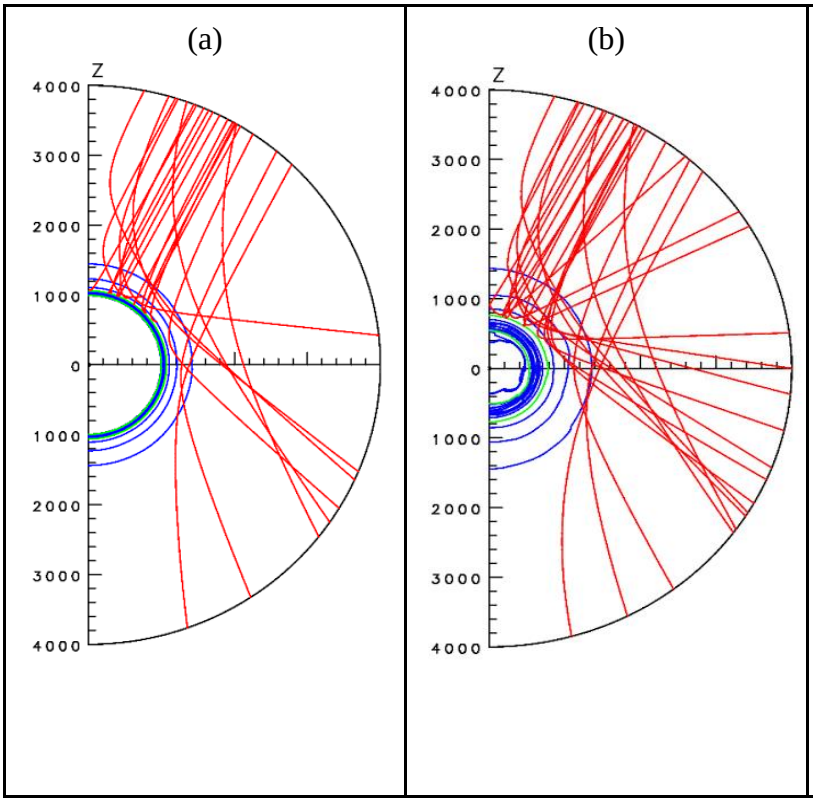

Figure 13: Raytrace plots of a quad 2 beam on the first oblique design at (a) 2 nanoseconds and (b) 6 nanoseconds. (a) At early times, this beam with a large defocus and oblique pointing still transfers most of its energy to the target. (b) As time progresses, more of the energy from this beam misses the target, contributing to lower absorption. With oblique shifts, each ray is depositing its energy over a larger portion of the target as it refracts through the plasma, which may help to reduce the effects of laser speckle on uniformity.

A second oblique design was developed using large pointing shifts with smaller defocuses in an attempt to increase the energy absorption of the implosion. For example, the quad 1 defocuses are 2.0 cm in this design, in comparison with 3.0 cm in the first oblique design. While only about 1% energy absorption was regained with this type of design, the smaller defocuses may help to reduce the speckle present in each beam, because individual beam speckle gets worse as the defocus increases. Therefore, smaller defocuses are also advantageous for creating a uniform implosion. Because there wasn't much gain in absorption with this design, a 25% increase in energy on all beams was still used. If this type of design proves viable on the NIF, phase plates could be developed that allow oblique beams with greater absorption. This design is shown in Figure 14 and has an RMS nonuniformity of 0.64%.

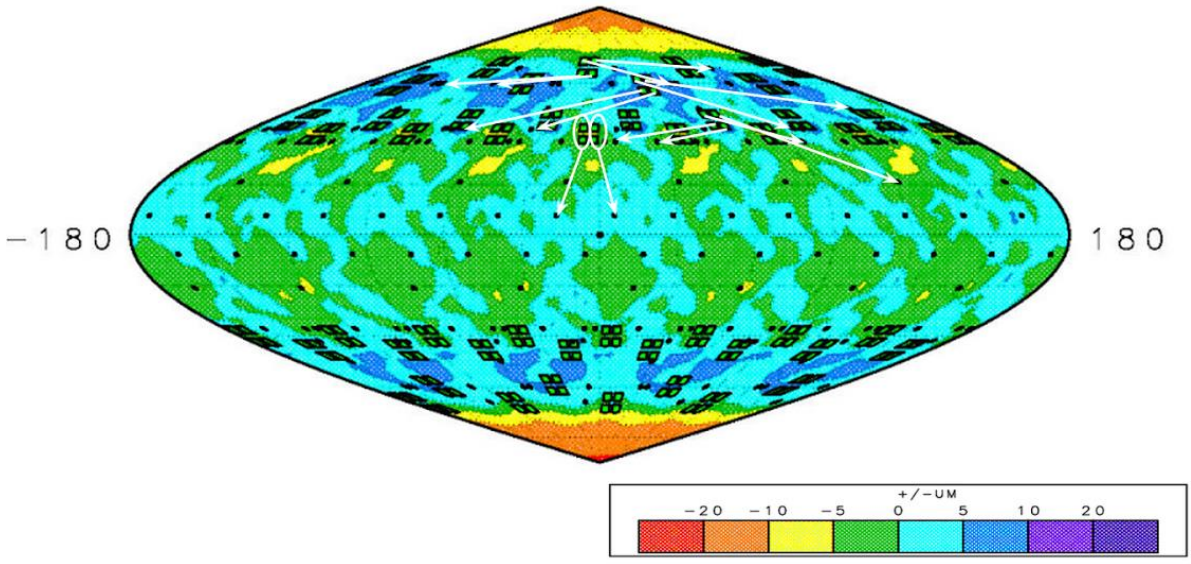

Figure 14: *SAGE* center-of-mass radius contour plot showing deviations from the mean radius in μm and pointings of the second oblique design when the target has been compressed to 631 μm. This design has an RMS nonuniformity of 0.64%.

One significant advantage of all of these designs is the reduction of the azimuthal nonuniformity at Θ=60° seen in the current design. As seen in figure 15, both the defocused and the first oblique design decrease the azimuthal rms nonuniformity at Θ=60° by close to a factor of two, significantly improving the overall uniformity of the implosion.

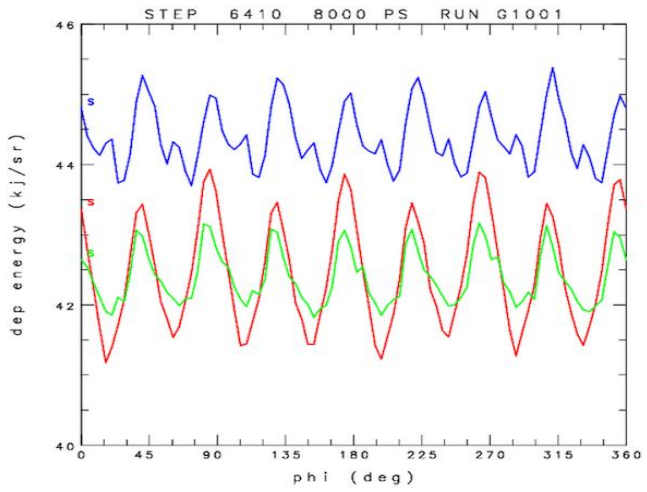

Figure 15: Lineout at Θ=60° of deposited energy vs Φ for the current design (red, rms = 1.84%), the defocused design (green, rms = 0.91%), and the first oblique design (blue, rms = 0.97%). Both the defocused design and the oblique design improve upon the rms nonuniformity of the current design at this Θ by a factor of 2.

4 c. Overdriven Equator Designs

A final set of designs was developed with the goal of overdriving the equator of the target. Adequately driving the equator has been a persistent problem with polar drive experiments. In order to test the accuracy of the *SAGE* and *DRACO* hydrodynamics codes in modeling the amount of drive at the equator and to allow for adjustments to the equatorial drive based on experimental data, two designs were developed that overdrive the equator. These designs also demonstrate the ability of polar drive to significantly overdrive the equator. The first design overdrives the equator by about 5%, and the second design overdrives the equator by about 10%. Both of these designs use large defocuses on the poles and small defocuses on the equator along with comparatively more energy on the quad 4 beams. As seen in figure 16, both designs overdrive the equator in a relatively smooth manner, and the design that overdrives the

equator by 5% overdrives the equator more gently than the second design. It hasn't been observed in experiments that the equator is 10% under compressed in relation to the poles [Figure 6], but the purpose of the 10% overdriven design is to show that the equator can be over compressed in a polar drive experiment.

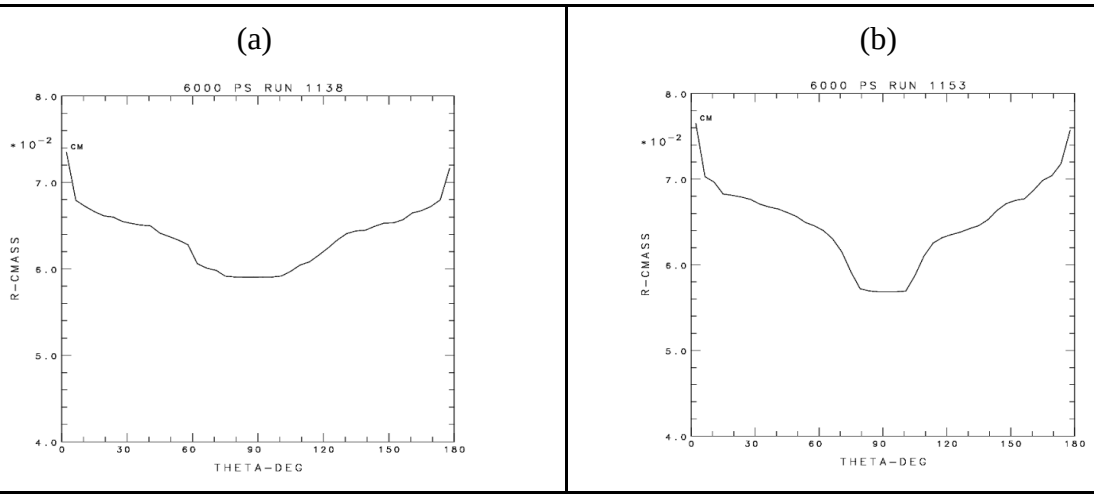

Figure 16: Center-of-mass radius in cm vs Θ, averaged over Φ, for both overdriven equator designs. (a) The equator is overdriven by about 5%. (b) The equator is overdriven by about 10%.

5. Conclusion

Several new designs for polar drive implosions on the NIF were developed using the hydrodynamics code *SAGE*. A design utilizing larger defocuses to improve uniformity gave an rms nonuniformity of 0.64%. Two oblique designs, one with larger defocuses and one with smaller defocuses, were also developed that gave good uniformity using large pointing shifts. It is speculated that these large pointing shifts could help reduce the effect of laser speckle on the uniformity of NIF polar drive implosions. Additionally, two designs were developed that overdrive the equator of the target to allow for tuning of polar drive implosions based on experimental data. All of the designs are straightforward to test on the NIF.

6. Acknowledgements

First, I would like to thank Mrs. Shayne Watterson for telling me about the High School Program and for encouraging me to apply. I would also like to thank my parents for their support. Finally, I would like to thank Dr. Craxton both for organizing the High School Program and for all of his help and support with my project.

7. References

1. Yifan Kong, *"Beam-Pointing Optimization for Proton Backlighting on the NIF,"* Laboratory for Laser Energetics High School Summer Research Program (2013).
2. J. Nuckolls et al., *"Laser Compression of Matter to Super-High Densities: Thermonuclear (CTR) Applications,"* Nature 239, 139 (1972).
3. J. D. Lindl, *"Development of the Indirect-Drive Approach to Inertial Confinement Fusion and the Target Basis for Ignition and Gain,"* Phys. Plasmas 2, 3933 (1995).
4. S. Skupsky et al., *"Polar Direct Drive on the National Ignition Facility,"* Phys. Plasmas 11, 2763 (2004).
5. A. M. Cok et al., *"Polar-drive designs for optimizing neutron yields on the National Ignition Facility,"* Phys. Plasmas 15, 082705 (2008).
6. R. S. Craxton et al., *"Polar direct drive: Proof-of-principle experiments on OMEGA and prospects for ignition on the National Ignition Facility,"* Phys. Plasmas 12, 056304 (2005).
7. P. B. Radha et al., *"Polar-drive implosions on OMEGA and the National Ignition Facility,"* Phys. Plasmas 20, 056306 (2013).

8. Alexandra M. Cok, *"Development of Polar Direct Drive Designs for Initial NIF Targets,"* Laboratory for Laser Energetics High School Summer Research Program (2006).

9. D. T. Michel, private communication.

10. F. J. Marshall, private communication.